

Lennard-Jones as a model for argon and test of extended renormalization group calculations

John A. White

Department of Physics, American University, Washington, DC 20016-8058

(Received 14 June 1999; accepted 30 August 1999)

Renormalization group (RG) procedures have been extended recently in phase-space cell approximation to predict, in addition to universal thermal properties observed asymptotically close to the gas-liquid critical point of fluids, also nonuniversal and nonasymptotic properties. This “globalized” RG theory is applied here, using a Lennard-Jones potential, to calculate the temperature, density, and pressure at the critical point of argon and to calculate pressures for a wide range of densities at temperatures close to, below, and considerably above that at the argon critical point. Choices required for the Lennard-Jones parameters and the quality of fit to experimental data suggest some of the strengths and limitations of the global RG theory. © 1999 American Institute of Physics. [S0021-9606(99)50744-7]

I. INTRODUCTION

The Lennard-Jones 12-6 potential has been much investigated as a simple, approximate model for intermolecular interactions in fluids. Using that potential, it should be possible to construct an accurate global statistical mechanical theory of thermal properties of the Lennard-Jones fluid to compare with properties observed over wide ranges of densities and temperatures in some real fluids. But for “Lennard-Jonesium,” as for other model fluids with attractive intermolecular interactions of limited range, taking properly into account transient, spontaneous deviations from average density—which contribute significantly to thermal properties for densities and temperatures in a large neighborhood of the gas-liquid critical point—has not proven to be easy to do.

The difficulty in taking these spontaneous thermal fluctuations into account in the theory is that different Fourier components of the fluctuations tend all to interact with one another. A general, renormalization group (RG) procedure for treating fluctuations of different wavelengths that interact with one another was developed in 1971 by K. Wilson.¹ The theory was developed for use in the limit that the shortest wavelengths of interest are long compared with the range of the relevant intermolecular forces. Wilson’s work led to several predictions regarding thermal behavior that is independent of details of intermolecular interactions, such as occurs when the Curie point of an Ising model magnet or critical point of a fluid is approached closely.

In the past few years, some suggestions have been made for extending the theory, in phase-space cell approximation, to include contributions from shorter wavelength fluctuations and to take into account details of the intermolecular interactions.^{2,3} The goal of this work has been to arrive at a global renormalization group theory that is applicable throughout all or much of the gas and liquid phases of fluids and that predicts their thermal properties to good accuracy

from a knowledge solely of relevant microscopic intermolecular interactions.

The basic phase-space cell approximation employed in Refs. 2 and 3 was essentially that introduced originally by Wilson¹ to provide simple, qualitative and only semiquantitative insights. Subsequently, Wilson and others developed more accurate, field theoretic methods that give better quantitative agreement with behavior observed asymptotically close to critical points. But to date it appears not to have been possible to extend these field-theoretic methods globally to treat fluctuations of arbitrarily short wavelength to predict thermal behavior accurately to far from the critical point. Nor, even at the critical point, has it proved possible to date to calculate accurately by the field-theoretic methods several nonuniversal properties – including the critical point pressure, density, and temperature – that depend on details of the intermolecular potentials.

The present investigation was undertaken in an effort to understand better the strengths and limitations of RG theory in phase-space cell approximation when extended to make thermal property predictions both at and to far from the critical point by taking into account nonuniversal properties and fluctuations at all wavelengths. Because good experimental pressure isotherm data is available for a rather wide range of densities and temperatures about the argon critical point,⁴ this investigation has focused on argon as a testing ground for the theory, using the Lennard-Jones potential as model for the intermolecular interactions among the argon atoms.⁵

In the following, the equations used to calculate the thermal properties of the Lennard-Jones fluid are summarized in Sec. II. Results obtained for specific choices for the two Lennard-Jones parameters are discussed in Sec. III, together with some quantitative statements regarding choices of shortest fluctuation wavelength and size of fluctuation averaging volume used in the phase-space cell approximation. A statement of conclusions follows, in Sec. IV.

II. METHOD OF CALCULATION

A. Two-body potential, mean-field approximation, treatment of repulsive interactions

The Lennard-Jones 12-6 potential is a spherically symmetric two-body intermolecular potential of the form

$$U(r) = U_{LJ}(r) = 4\epsilon(x^{-12} - x^{-6}), \quad x = r/\sigma, \quad (1)$$

where r is the separation between molecular centers, ϵ is the maximum depth of the potential well, and $r = \sigma$ is where the potential changes sign from positive to negative. The renormalization group procedure developed for fluids^{2,3} treats the steeply repulsive and more slowly varying attractive portions of the potential separately, with renormalization procedures employed only for the attractive part.

At very high temperatures, contributions from renormalization are quite small and the free energy density (Helmholtz free energy per unit volume) $f(T, \rho)$ is approximately

$$f(T, \rho) \approx f_{\text{repulsive}} - a(T, \rho)\rho^2, \quad (2)$$

where ρ is the number of molecules per unit volume and

$$a(T, \rho) = \int_{\Omega} d\mathbf{r} U_2(r) g_{\text{repulsive}}(T, \rho, r). \quad (3)$$

Here $U_2(r)$ is one-half the attractive part of the pair potential, $g_{\text{repulsive}}$ is the radial distribution function for the repulsive interactions, and Ω is the domain of integration, assumed to extend to large values of $x = r/\sigma$.

In the present investigation, the $f_{\text{repulsive}}$ was taken to be that for a gas of hard spheres in Carnahan–Starling approximation⁶

$$\rho \frac{\partial}{\partial \rho} \left(\frac{\beta f_{\text{repulsive}}}{\rho} \right) = Z_{\text{repulsive}} = \frac{1 + y + y^2 - y^3}{(1 - y)^3}, \quad (4)$$

from which

$$\frac{\beta f_{\text{repulsive}}}{\rho} = \frac{4y - 3y^2}{(1 - y)^2} + \ln y, \quad (5)$$

plus a contribution dependent on temperature but independent of density that is not needed here. (It produces a non-vanishing specific heat at constant density but does not contribute to the pressure, given by $P = \rho \partial f / \partial \rho - f$.) In the above, $Z = PV/RT = \beta P/\rho$, where $\beta = 1/k_B T$ is the reciprocal of the temperature multiplied by Boltzmann's constant k_B , and $y = \frac{1}{6}\pi\rho d^3$. The diameter d of the molecular cores was chosen to be⁷

$$\begin{aligned} d(T) &= \int_0^\sigma (1 - e^{-\beta U_L - J(r)}) dr \\ &= \sigma \int_0^1 (1 - e^{-4\epsilon\beta(x^{-12} - x^{-6})}) dx \end{aligned} \quad (6)$$

and the $g_{\text{repulsive}}(T, \rho, r)$, used also below in Eq. (15), was evaluated for hard spheres of diameter $d(T)$ in Percus–Yevick approximation.^{8,9}

B. Renormalization corrections to mean field approximation for the attractive interactions

To correct Eq. (2) for fluctuation enhancements at lower temperatures in the presence of the attractive potential (because nonuniform densities are energetically favored) a global renormalization procedure was used to find successively improved expressions, as n , and the fluctuation wavelengths $\lambda \approx \lambda_n$, increase:

$$f(T, \rho) \approx f_n(T, \rho) - a(T, \rho)\rho^2, \quad (7)$$

where, for each $n (> 0)$,

$$f_n(T, \rho) = f_{n-1}(T, \rho) + \delta f_n(T, \rho), \quad (8)$$

and

$$f_0(T, \rho) = f_{\text{repulsive}}(T, \rho). \quad (9)$$

The increment $\delta f_n(T, \rho)$ at each order $n = 1, 2, 3, \dots$ was taken to be^{2,3}

$$\delta f_n(T, \rho) = \frac{1}{\beta V_n} \ln \frac{I_{n,s}(T, \rho)}{I_{n,l}(T, \rho)}, \quad (10)$$

where V_n is the volume within which, in the phase-space cell approximation, fluctuations of wavelength $\lambda \approx \lambda_n$ are averaged. In Eq. (10), the $I_{n,s}(T, \rho)$ and $I_{n,l}(T, \rho)$ are integrals over the amplitudes of the wavepackets of fluctuations of wavelengths $\lambda \approx \lambda_n$:

$$I_{n,i}(T, \rho) = \int_0^{\rho'} dx e^{-\beta V_n D_{n,i}(T, \rho, x)}, \quad i = s, l. \quad (11)$$

The upper density limit, ρ' , is the smaller of ρ or $\rho_{\text{max}} - \rho$, where ρ_{max} does not exceed the density of close packing. Each $D_{n,i}(T, \rho, x)$ is given by

$$\begin{aligned} 2D_{n,i}(T, \rho, x) &= \hat{f}_{n-1,i}(T, \rho + x) + \hat{f}_{n-1,i}(T, \rho - x) \\ &\quad - 2\hat{f}_{n-1,i}(T, \rho), \end{aligned} \quad (12)$$

where, for $i = l$,

$$\hat{f}_{n-1,l}(T, \rho) = f_{n-1}(T, \rho), \quad (13)$$

and for $i = s$,

$$\hat{f}_{n-1,s}(T, \rho) = f_{n-1}(T, \rho) - a_n(T, \rho)\rho^2. \quad (14)$$

The $a_n(T, \rho)$ in Eq. (14) is the cosine Fourier transform of the product $U_2(r)g_{\text{repulsive}}(T, \rho, r)$,

$$a_n(T, \rho) = \int_{\Omega} d\mathbf{r} \cos(\mathbf{k}_n \cdot \mathbf{r}) U_2(r) g_{\text{repulsive}}(T, \rho, r), \quad (15)$$

for a (sinusoidal) wave of wavelength $\lambda_n = 2\pi/k_n$.

In the limit $n \rightarrow \infty$, for which $\lambda_n \rightarrow \infty$, the $a_n(T, \rho)$ given by Eq. (15) becomes simply the $a(T, \rho)$ in Eqs. (2) and (7) above. And in the limit $\beta \rightarrow 0$ the corrections $\delta f_n(T, \rho)$ given by Eq. (10) all vanish, so that Eq. (7) then becomes equivalent to Eq. (2).

The above renormalization group equations are capable of determining the free energy density completely, by taking fully into account details of the intermolecular potential and contributions made by fluctuations at all wavelengths rather than limiting just to aspects of contributions made by fluc-

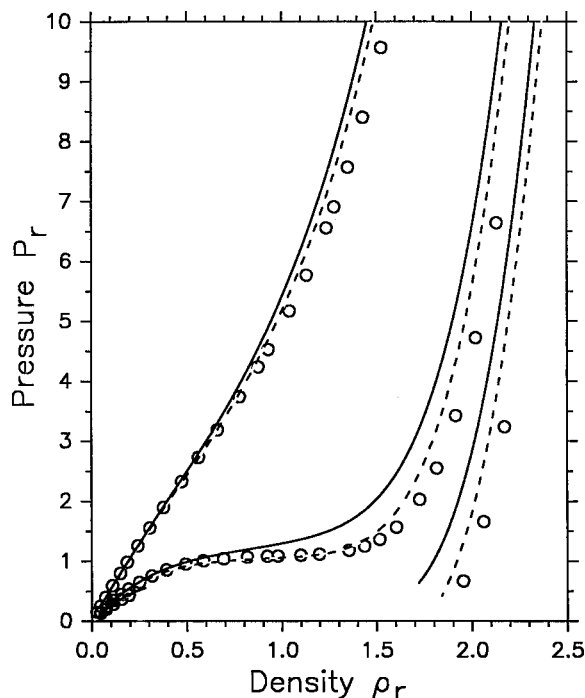


FIG. 1. Pressure isotherms for argon at temperatures $T_r=0.883, 1.015, 1.645$. Open circles: results of measurements (Ref. 4). Solid and dashed lines: theoretical predictions for two choices of the Lennard-Jones parameters σ and ϵ (see text). Temperatures, densities, and pressures are all given relative to the T_c , ρ_c , P_c at the critical point as determined by the measurements (Ref. 4).

tuations of asymptotically long wavelengths. Their derivation is discussed elsewhere,^{2,3} though a somewhat cruder approximation than Eqs. (14) and (15) above was used in that earlier work [Eqs. (8) and (9) in Ref. 3]. As shown previously (Ref. 3 and Sec. IIB of Ref. 10), when one is sufficiently close to the critical point and for asymptotically long wavelengths λ_n , the equations above become equivalent to the renormalization relations in phase-space cell approximation that were derived originally for an Ising model ferromagnet.^{1,11}

For the calculations reported below, the wavelengths λ_n used in Eq. (15) were chosen to have the values $\lambda_n = \lambda_1 t^{n-1}$, with $\lambda_1 = 4\sigma$ and $t=2$, and the averaging volumes V_n used in Eqs. (10) and (11) were chosen, at each n , to be of size $V_n = (z\lambda_n/2)^\Delta$, with $z \approx 1$ and dimensionality $\Delta=3$. Values for the constants λ_1 and z are not, and need not be, specified for RG calculations of critical point exponents^{1,11} but need to be known for global RG calculations that provide predictions of nonuniversal properties at the critical point and of thermal behavior to sizable distances away from the critical point. In particular, the choice $\lambda_1 \approx 4\sigma$ ensures that fluctuations of all wavelengths that make appreciable contributions to Eq. (15) are taken into account. And the choice $z \approx 1$ results in each averaging volume V_n being not much smaller than wavepackets consisting of density fluctuations of wavelengths $\lambda \approx \lambda_n$, while at the same time small enough that variations of density at wavelengths $\lambda \geq 2\lambda_n$ can be expected to contribute relatively little to the increment of free energy, $\delta f_n(T, \rho)$, calculated for the fluctuations of wavelength $\lambda \approx \lambda_n$.

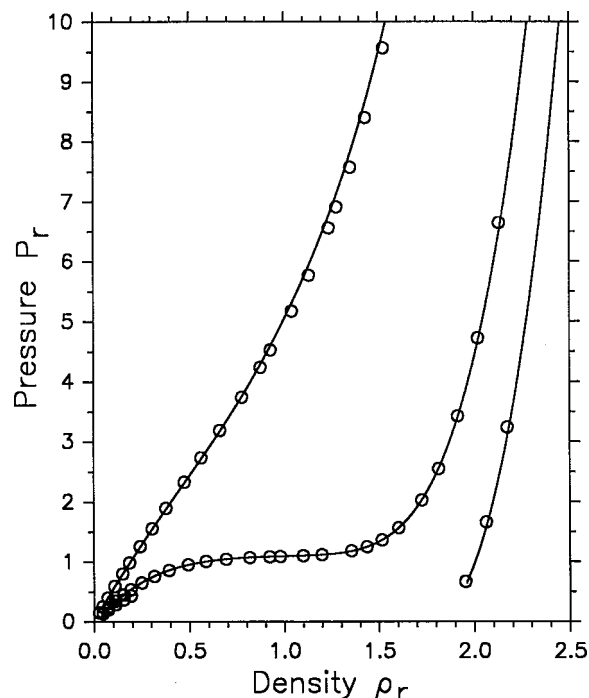


FIG. 2. Calculated pressure isotherms compared with experiment for the same three temperatures as in Fig. 1, now for $\sigma=3.405 \text{ \AA}$, $\epsilon/k_B=118.2 \text{ K}$, for attractive potential assumed to begin at $r=d'=(d+\sigma)/2$ instead of at $r=d$.

For most of the work reported below the coefficients λ_1 and z were simply assigned the values $\lambda_1=4\sigma$ and $z=1$.

III. SOME CALCULATIONAL DETAILS

In the numerical calculations, the integrations were performed by trapezoid rule, using equal size steps. Typically, 1000 steps were used for the calculation of the hard-sphere diameter d in Eq. (6) and also, for values $1 \leq r/d \leq 10$, for the calculation of each $a_n(T, \rho)$, in Eq. (15). For the $g_{\text{repulsive}}(T, \rho, r)$ appearing in Eq. (15), tables in Refs. 7 and 8 were used, with interpolation when required, for values $r/d \leq 6$. For $r/d > 6$, the approximation $g_{\text{repulsive}}=1$ was employed, which is probably a good approximation for such large values of r/d . Equation (15) was evaluated for the twelve (dimensionless) densities $\rho d^3 = 0.0, 0.1, 0.2, \dots, 1.1$ for which tabulated values of $g_{\text{repulsive}}$ were available, and a polynomial of fifth order in ρd^3 was fitted to each $a_n(T, \rho)$ for use in Eq. (14) at other than those twelve densities.

The free energy density f was then evaluated, at (dimensionless, ρd^3) density intervals of 0.005, for $0 < \rho d^3 \leq 1.1$; for the lower limit, a small value, $\rho d^3 = 5 \times 10^{-12}$, was used in place of $\rho d^3 = 0$ to avoid the logarithmic singularity in Eq. (5). The integrand in (11) was evaluated at the same dimensionless density intervals, 0.005, using for the maximum integration limit $\rho' d^3 = \rho_{\text{max}} d^3 / 2 = 1.1/2$. Smaller choices for that limit, down to $\rho' d^3 = 0.9/2$, had almost no noticeable effect on the results obtained here. Results obtained were found to change only a little when the density steps used in evaluating f were made twice as big, to intervals of 0.01, and to change negligibly, for present purposes, for smaller steps.

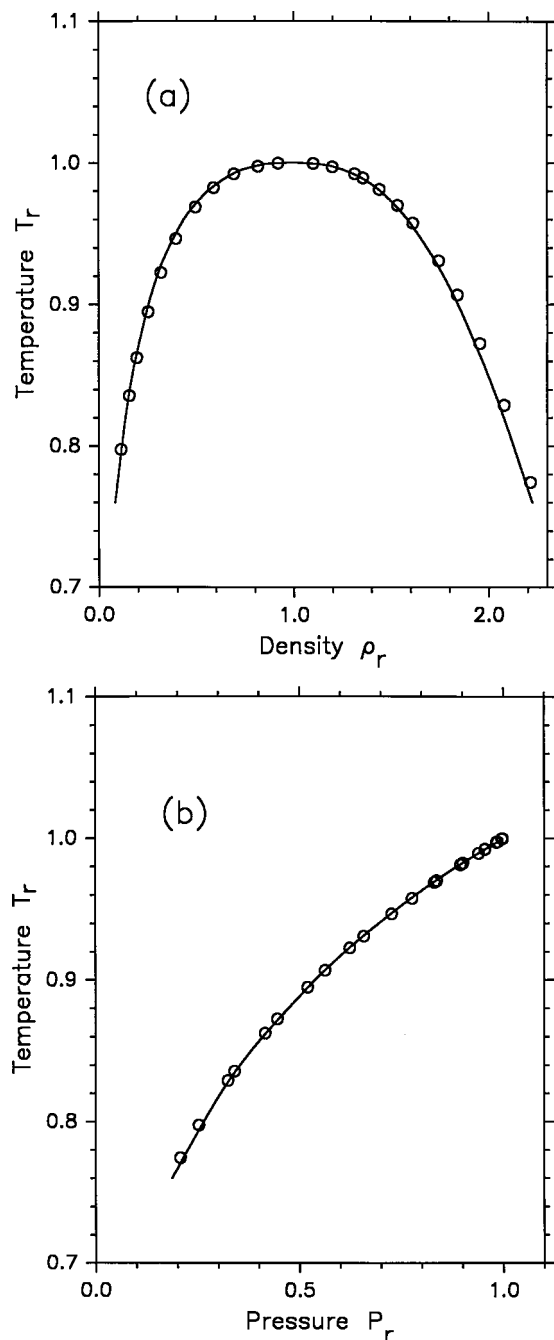


FIG. 3. Coexisting gas and liquid densities (a), and vapor pressures (b), predicted for the d' used in Fig. 2 and the choices of σ and ϵ that give exactly the measured (Ref. 4) critical point temperature and density (see text). Open circles are results of measurements from Table VI in Ref. 4.

Four point interpolation was used to estimate f when calculating thermal properties at densities intermediate between those at which f had been evaluated.

Calculations of $f_n(T, \rho)$ were carried through to order $n=6$. After the first few iterations of the recursion relations for increasing n , contributions δf_n decreased rapidly in size, with, for present purposes, negligible contributions for $n > 6$.

IV. RESULTS

In carrying through the calculations described in the previous section, the “attractive” part of the potential was taken

initially to be the U_{LJ} of Eq. (1) for all $r > d$, for d given by Eq. (6). For all $r < d$, the $U_2(r)$ in Eqs. (15) and (3) was set equal to zero. Using $\lambda_1 = 4\sigma$ and $z = 1$, the $f(T, \rho)$ given by Eq. (7) was then completely determined, apart from a contribution dependent only on temperature that does not contribute to the pressure [see Eq. (5)], upon assigning values to the LJ parameters, σ and ϵ .

Figure 1 shows pressures calculated for argon for two different choices for the Lennard-Jones parameters σ and ϵ and comparison measured pressures,⁴ at three temperatures $T/T_c = 0.883$, 1.015, and 1.645. The solid lines are for¹² $\sigma = 3.405$ Å, $\epsilon/k_B = 119.8$ K. The root mean square deviation – of perpendicular distances between the measured points (open circles) and theoretical curves – for the solid curves is 9.7%. The dashed curves are for another choice for the LJ parameters for argon:¹³ $\sigma = 3.405$ Å, $\epsilon/k_B = 125.2$ K. The rms deviation for those curves is 2.8%.

A third choice, not shown in Fig. 1, is¹⁴ $\sigma = 3.504$ Å, $\epsilon/k_B = 117.7$ K. It gives better overall agreement with second virial coefficient measurements in argon,¹⁵ but results in a larger rms deviation, 12.4%, for the set of data points shown in Fig. 1.

Finally, a fourth choice for σ and ϵ , one that gives better results than is shown in Fig. 1, is $\sigma = 3.345$ Å, $\epsilon/k_B = 125.7$ K, with rms deviation between theory and experiment now 1.1%. This choice of values for σ and ϵ results in exact agreement between the calculated critical point density and temperature and the values, $\rho_c = (1/123.81 \text{ Å}^3)$ and $T_c = 150.86$ K, determined from the measurements.⁴

From the above, it can be seen that calculated results are quite sensitive to the choices of σ and ϵ : the ϵ values used were all within 7% of one another, and the σ values within 5%. Calculated results were also found to be somewhat, but not equally, sensitive to the assignments $\lambda_1 = 4\sigma$, $z = 1$. For example, for the solid curves in Fig. 1, a $\pm 20\%$ change in λ_1 or $\pm 8\%$ change in z causes about $\pm 1\%$ change in the rms deviation [i.e., to $(9.7 \pm 1)\%$].

V. CONCLUSIONS

It appears from the above that, for argon, and for the choices $\lambda_1 = 4\sigma$, $z = 1$, the combined errors of approximation, resulting from use of a Lennard-Jones type potential and a phase-space cell approximation in the renormalization calculations, can be largely compensated by making an adjustment of several percent in values chosen for the Lennard-Jones parameters σ and ϵ . Once that has been done, predicted pressures agree with those measured in argon to $\sim 1\%$ over a wide range of densities and temperatures that includes the critical point.

It should be kept in mind, however, that the above is yet a rather crude test of the renormalization procedure used. The Lennard-Jones is strictly a two-body potential and ignores nonadditive contributions, such as are discussed in Ref. 16. Even where such nonadditive contributions make negligible contributions, at densities on the extreme left in Fig. 1 that are used for the calculation of second virial coefficients, the – two parameter – Lennard-Jones form of potential is known to be less accurate than potentials that in-

clude a third parameter.¹⁴ Thus the good agreement with the measurements of Ref. 4 to $\sim 1\%$ rms error over a wide range of densities and temperatures for a suitable choice of Lennard-Jones parameters σ and ϵ , e.g., the above “fourth choice,” could be a result of a fortuitous cancellation of errors which individually are considerably larger.

Additionally, what numbers should be used for σ and ϵ for good results depends on how the potential has been separated into attractive and repulsive parts. For example, the repulsive part of the potential might be treated as in Sec. II A above but the attractive part taken to be of Lennard-Jones form beginning, not at $r=d$ as in Sec. III, but at $r=d'$, with d' somewhere between $d(T)$ and σ .

In particular, d' could be chosen to be $d'=(d+\sigma)/2$, i.e., exactly half-way between $d(T)$ and σ , and $U_2(r)$ in Eqs. (15) and (3) set equal to zero for all $r<d'$. In that case, when $\lambda_1=4\sigma$ and $z=1$, the rms deviation between the calculated and measured pressures at the same three temperatures as in Fig. 1 becomes 2.9% for¹² $\sigma=3.405$, $\epsilon/k_B=119.8$ and approximately 1% (more exactly, 0.75%) for the choice $\sigma=3.405$ Å, $\epsilon/k_B=118.2$ K. Calculated pressure isotherms for the latter choice of σ and ϵ are shown in Fig. 2.

For the same choice of $d'=(d+\sigma)/2$, $\lambda_1=4\sigma$, $z=1$, the σ and ϵ values that give exactly the measured⁴ T_c and ρ_c are now $\sigma=3.419$ Å, $\epsilon/k_B=117.8$ K, with rms deviation 1.2%. Figures 3(a) and 3(b) show the gas and liquid densities and vapor pressures calculated in the two-phase region below the critical point temperature for this choice of σ and ϵ .

Finally, for $\lambda_1=4\sigma$, $z=1$, but $d'=\sigma$, with $U_2(r)=0$ for all $r<\sigma$, the σ , ϵ/k_B that give the measured T_c , ρ_c are 3.487 Å, 111.7 K, with rms deviation 2.3%; and the rms deviation becomes 1.0% for $\sigma=3.46$ Å, $\epsilon/k_B=112.7$ K.

¹K. G. Wilson, Phys. Rev. B **4**, 3184 (1971).

²J. A. White and S. Zhang, J. Chem. Phys. **99**, 2012 (1993).

³J. A. White and Sheng Zhang, Int. J. Thermophys. **19**, 1019 (1998).

⁴A. Michels, J. M. Levelt, and W. DeGraaff, Physica (Amsterdam) **24**, 659 (1958).

⁵Some alternative theoretical approaches for calculating volumetric properties of argon and/or Lennard-Jones fluids throughout a large neighborhood of the critical point have been discussed, with references to earlier work, in T. Kraska and U. K. Deiters, Int. J. Thermophys. **15**, 261 (1994); M. Tau, A. Parola, D. Pini, and L. Reatto, Phys. Rev. E **52**, 2644 (1995); L. Reatto and A. Parola, J. Phys.: Condens. Matter **8**, 9221 (1996); Y. Tang, J. Chem. Phys. **109**, 5935 (1998).

⁶N. F. Carnahan and K. E. Starling, J. Chem. Phys. **51**, 635 (1969).

⁷J. A. Barker and D. Henderson, J. Chem. Phys. **47**, 4714 (1967).

⁸G. J. Throop and R. J. Bearman, J. Chem. Phys. **42**, 2408 (1965).

⁹F. Mandel, R. J. Bearman, and M. Y. Bearman, J. Chem. Phys. **52**, 3315 (1970).

¹⁰J. A. White and S. Zhang, J. Chem. Phys. **103**, 1922 (1995).

¹¹K. G. Wilson and M. E. Fisher, Phys. Rev. Lett. **28**, 240 (1972).

¹²A. Michels, H. Wijk, and H. Wijk, Physica (Amsterdam) **15**, 627 (1949).

¹³B. E. F. Fender and G. D. Halsey, Jr., J. Chem. Phys. **16**, 1881 (1962).

¹⁴A. E. Sherwood and J. M. Prausnitz, J. Chem. Phys. **41**, 429 (1964).

¹⁵Fitting to second virial coefficient data for argon as in Ref. 14, Sherwood, private communication, has found that the overall rms deviations of the calculated second virial coefficients for temperatures in the full range 85–873 K are in the ratio approximately 1/1.7/2.8 for the σ, ϵ choices in Refs. 14, 13, and 12, respectively. For the three particular temperatures used for Fig. 1, the individual deviations are of roughly equal magnitude for the σ and ϵ of Refs. 14 and 12, but, at the upper two temperatures, considerably larger for the σ and ϵ from Ref. 13. [The choices of σ and ϵ in Refs. 13 and 12 work best in different temperature regimes: deviations from measured second virial coefficients for the σ and ϵ of Ref. 13 are generally larger than for the other two choices of σ, ϵ for temperatures above $0.9T_c$, but smallest for temperatures below 90 K; while the σ and ϵ of Ref. 12 give generally the smallest deviations for temperatures higher than T_c (≈ 151 K), but especially large deviations for temperatures below about $0.9T_c$.] I wish to thank A. E. Sherwood for providing me with tabulations of calculated second virial coefficients for the Lennard-Jones potential applied to argon, and their deviations from values derived from experiment, for the temperatures and σ, ϵ values mentioned above.

¹⁶B. M. Axilrod and E. Teller, J. Chem. Phys. **11**, 299 (1943).